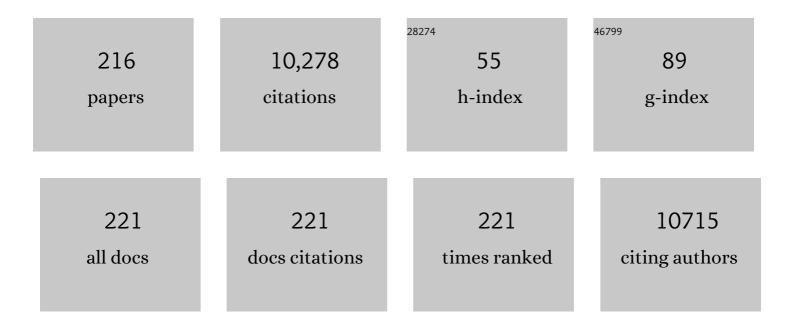
## Lih-Sheng Turng

List of Publications by Year in descending order

Source: https://exaly.com/author-pdf/1448014/publications.pdf Version: 2024-02-01



#	Article	IF	CITATIONS
1	Highly Stretchable and Biocompatible Strain Sensors Based on Mussel-Inspired Super-Adhesive Self-Healing Hydrogels for Human Motion Monitoring. ACS Applied Materials & Interfaces, 2018, 10, 20897-20909.	8.0	398
2	Biocompatible, self-healing, highly stretchable polyacrylic acid/reduced graphene oxide nanocomposite hydrogel sensors via mussel-inspired chemistry. Carbon, 2018, 136, 63-72.	10.3	282
3	Highly compressible ultra-light anisotropic cellulose/graphene aerogel fabricated by bidirectional freeze drying for selective oil absorption. Carbon, 2018, 132, 199-209.	10.3	278
4	Mussel-inspired electroactive chitosan/graphene oxide composite hydrogel with rapid self-healing and recovery behavior for tissue engineering. Carbon, 2017, 125, 557-570.	10.3	253
5	Characterization of thermoplastic polyurethane/polylactic acid (TPU/PLA) tissue engineering scaffolds fabricated by microcellular injection molding. Materials Science and Engineering C, 2013, 33, 4767-4776.	7.3	235
6	High-performance flexible triboelectric nanogenerator based on porous aerogels and electrospun nanofibers for energy harvesting and sensitive self-powered sensing. Nano Energy, 2018, 48, 327-336.	16.0	205
7	Highly transparent, stretchable, and rapid self-healing polyvinyl alcohol/cellulose nanofibril hydrogel sensors for sensitive pressure sensing and human motion detection. Sensors and Actuators B: Chemical, 2019, 295, 159-167.	7.8	199
8	Fabrication of scaffolds in tissue engineering: A review. Frontiers of Mechanical Engineering, 2018, 13, 107-119.	4.3	183
9	Highly Efficient Removal of Methylene Blue Dye from an Aqueous Solution Using Cellulose Acetate Nanofibrous Membranes Modified by Polydopamine. ACS Omega, 2020, 5, 5389-5400.	3.5	170
10	Crystalline Morphology of Electrospun Poly(ε-caprolactone) (PCL) Nanofibers. Industrial & Engineering Chemistry Research, 2013, 52, 4939-4949.	3.7	153
11	A review of current developments in process and quality control for injection molding. Advances in Polymer Technology, 2005, 24, 165-182.	1.7	152
12	Effects of annealing time and temperature on the crystallinity and heat resistance behavior of injectionâ€molded poly(lactic acid). Polymer Engineering and Science, 2013, 53, 580-588.	3.1	152
13	Processing and characterization of solid and microcellular poly(lactic) Tj ETQq1 1 0.784314 rgBT /Overlock 10 1 Part B: Engineering, 2013, 51, 79-91.	f 50 267 T 12.0	d (acid)/poly 142
14	Incorporation of poly(ethylene glycol) grafted cellulose nanocrystals in poly(lactic acid) electrospun nanocomposite fibers as potential scaffolds for bone tissue engineering. Materials Science and Engineering C, 2015, 49, 463-471.	7.3	137
15	The surface grafting of graphene oxide with poly(ethylene glycol) as a reinforcement for poly(lactic) Tj ETQq1 1 Mechanical Behavior of Biomedical Materials, 2016, 53, 403-413.	0.784314 3.1	rgBT /Overlo 136
16	Microstructure and mechanical properties of microcellular injection molded polyamide-6 nanocomposites. Polymer, 2005, 46, 7273-7292.	3.8	133
17	Shish-Kebab-Structured Poly(ε-Caprolactone) Nanofibers Hierarchically Decorated with Chitosan–Poly(ε-Caprolactone) Copolymers for Bone Tissue Engineering. ACS Applied Materials & Interfaces, 2015, 7, 6955-6965.	8.0	126
18	Electrospinning thermoplastic polyurethane/graphene oxide scaffolds for small diameter vascular graft applications. Materials Science and Engineering C, 2015, 49, 40-50.	7.3	122

#	Article	IF	CITATIONS
19	Electrospun polycaprolactone/gelatin composites with enhanced cell–matrix interactions as blood vessel endothelial layer scaffolds. Materials Science and Engineering C, 2017, 71, 901-908.	7.3	119
20	Morphology and Properties of Injection Molded Solid and Microcellular Polylactic Acid/Polyhydroxybutyrate-Valerate (PLA/PHBV) Blends. Industrial & Engineering Chemistry Research, 2013, 52, 2569-2581.	3.7	118
21	Magnetically driven superhydrophobic silica sponge decorated with hierarchical cobalt nanoparticles for selective oil absorption and oil/water separation. Chemical Engineering Journal, 2018, 337, 541-551.	12.7	112
22	Poly(ε-caprolactone) (PCL)/cellulose nano-crystal (CNC) nanocomposites and foams. Cellulose, 2014, 21, 2727-2741.	4.9	107
23	The morphology, properties, and shape memory behavior of polylactic acid/thermoplastic polyurethane blends. Polymer Engineering and Science, 2015, 55, 70-80.	3.1	106
24	Quantitative study of shrinkage and warpage behavior for microcellular and conventional injection molding. Polymer Engineering and Science, 2005, 45, 1408-1418.	3.1	105
25	Study of injection molded microcellular polyamide-6 nanocomposites. Polymer Engineering and Science, 2004, 44, 673-686.	3.1	104
26	Triboelectric Nanogenerators Made of Porous Polyamide Nanofiber Mats and Polyimide Aerogel Film: Output Optimization and Performance in Circuits. ACS Applied Materials & Interfaces, 2018, 10, 30596-30606.	8.0	103
27	Microcellular injection-molding of polylactide with chain-extender. Materials Science and Engineering C, 2009, 29, 1258-1265.	7.3	100
28	A novel method of producing lightweight microcellular injection molded parts with improved ductility and toughness. Polymer, 2015, 56, 102-110.	3.8	100
29	In-situ fibrillated polytetrafluoroethylene (PTFE) in thermoplastic polyurethane (TPU) via melt blending: Effect on rheological behavior, mechanical properties, and microcellular foamability. Polymer, 2018, 134, 263-274.	3.8	98
30	Dual super-amphiphilic modified cellulose acetate nanofiber membranes with highly efficient oil/water separation and excellent antifouling properties. Journal of Hazardous Materials, 2020, 385, 121582.	12.4	96
31	Strong, Ductile Magnesium-Zinc Nanocomposites. Metallurgical and Materials Transactions A: Physical Metallurgy and Materials Science, 2009, 40, 3038-3045.	2.2	93
32	Artificial small-diameter blood vessels: materials, fabrication, surface modification, mechanical properties, and bioactive functionalities. Journal of Materials Chemistry B, 2020, 8, 1801-1822.	5.8	90
33	Processing and characterization of microcellular PHBV/PBAT blends. Polymer Engineering and Science, 2010, 50, 1440-1448.	3.1	89
34	Biocompatible, degradable thermoplastic polyurethane based on polycaprolactone-block-polytetrahydrofuran-block-polycaprolactone copolymers for soft tissue engineering. Journal of Materials Chemistry B, 2017, 5, 4137-4151.	5.8	89
35	A novel method for improving the surface quality of microcellular injection molded parts. Polymer, 2011, 52, 1436-1446.	3.8	87
36	Highly porous composite aerogel based triboelectric nanogenerators for high performance energy generation and versatile self-powered sensing. Nanoscale, 2018, 10, 23131-23140.	5.6	80

#	Article	IF	CITATIONS
37	Microstructure and crystallography in microcellular injection-molded polyamide-6 nanocomposite and neat resin. Polymer Engineering and Science, 2005, 45, 52-61.	3.1	79
38	Thermoplastic polyurethane/hydroxyapatite electrospun scaffolds for bone tissue engineering: Effects of polymer properties and particle size. Journal of Biomedical Materials Research - Part B Applied Biomaterials, 2014, 102, 1434-1444.	3.4	77
39	Electrospun aligned poly(propylene carbonate) microfibers with chitosan nanofibers as tissue engineering scaffolds. Carbohydrate Polymers, 2015, 117, 941-949.	10.2	76
40	Fabrication of poly(ε-caprolactone) tissue engineering scaffolds with fibrillated and interconnected pores utilizing microcellular injection molding and polymer leaching. RSC Advances, 2017, 7, 43432-43444.	3.6	75
41	Effects of nano-fillers and process conditions on the microstructure and mechanical properties of microcellular injection molded polyamide nanocomposites. Polymer Composites, 2003, 24, 655-671.	4.6	74
42	Microcellular processing of polylactide–hyperbranched polyester–nanoclay composites. Journal of Materials Science, 2010, 45, 2732-2746.	3.7	74
43	Comparison between PCL/hydroxyapatite (HA) and PCL/halloysite nanotube (HNT) composite scaffolds prepared by co-extrusion and gas foaming. Materials Science and Engineering C, 2017, 72, 53-61.	7.3	73
44	Highly filled biochar/ultra-high molecular weight polyethylene/linear low density polyethylene composites for high-performance electromagnetic interference shielding. Composites Part B: Engineering, 2018, 153, 277-284.	12.0	72
45	Processing and characterization of solid and microcellular PHBV/coir fiber composites. Materials Science and Engineering C, 2010, 30, 749-757.	7.3	69
46	Electrospinning of unidirectionally and orthogonally aligned thermoplastic polyurethane nanofibers: Fiber orientation and cell migration. Journal of Biomedical Materials Research - Part A, 2015, 103, 593-603.	4.0	69
47	Superhydrophobic Graphene/Cellulose/Silica Aerogel with Hierarchical Structure as Superabsorbers for High Efficiency Selective Oil Absorption and Recovery. Industrial & Engineering Chemistry Research, 2018, 57, 1745-1755.	3.7	69
48	Effects of nano- and micro-fillers and processing parameters on injection-molded microcellular composites. Polymer Engineering and Science, 2005, 45, 773-788.	3.1	68
49	A composite generator film impregnated with cellulose nanocrystals for enhanced triboelectric performance. Nanoscale, 2017, 9, 1428-1433.	5.6	67
50	Fabrication of triple-layered vascular grafts composed of silk fibers, polyacrylamide hydrogel, and polyurethane nanofibers with biomimetic mechanical properties. Materials Science and Engineering C, 2019, 98, 241-249.	7.3	67
51	Polylactide, nanoclay, and core–shell rubber composites. Polymer Engineering and Science, 2006, 46, 1419-1427.	3.1	66
52	Stretchable gelatin/silver nanowires composite hydrogels for detecting human motion. Materials Letters, 2019, 237, 53-56.	2.6	66
53	Improving surface quality of microcellular injection molded parts through mold surface temperature manipulation with thin film insulation. Polymer Engineering and Science, 2010, 50, 1281-1289.	3.1	65
54	Electrospun nanofibrous thermoplastic polyurethane/poly(glycerol sebacate) hybrid scaffolds for vocal fold tissue engineering applications. Materials Science and Engineering C, 2019, 94, 740-749.	7.3	64

#	Article	IF	CITATIONS
55	Morphology, mechanical properties, and mineralization of rigid thermoplastic polyurethane/hydroxyapatite scaffolds for bone tissue applications: effects of fabrication approaches and hydroxyapatite size. Journal of Materials Science, 2014, 49, 2324-2337.	3.7	60
56	Poly(ε-caprolactone) Nanofibers with a Self-Induced Nanohybrid Shish-Kebab Structure Mimicking Collagen Fibrils. Biomacromolecules, 2013, 14, 3557-3569.	5.4	59
57	In situ synthesis of polyurethane scaffolds with tunable properties by controlled crosslinking of tri-block copolymer and polycaprolactone triol for tissue regeneration. Chemical Engineering Journal, 2018, 348, 786-798.	12.7	58
58	Oxygen-Rich Polymers as Highly Effective Positive Tribomaterials for Mechanical Energy Harvesting. ACS Nano, 2019, 13, 12787-12797.	14.6	58
59	Nucleation Catalysis in Aluminum Alloy A356 Using Nanoscale Inoculants. Metallurgical and Materials Transactions A: Physical Metallurgy and Materials Science, 2011, 42, 2323-2330.	2.2	56
60	Promoting endothelial cell affinity and antithrombogenicity of polytetrafluoroethylene (PTFE) by mussel-inspired modification and RGD/heparin grafting. Journal of Materials Chemistry B, 2018, 6, 3475-3485.	5.8	56
61	Three-dimensional numerical simulation of injection molding filling of optical lens and multiscale geometry using finite element method. Polymer Engineering and Science, 2006, 46, 1263-1274.	3.1	54
62	Processing and characterization of recycled poly(ethylene terephthalate) blends with chain extenders, thermoplastic elastomer, and/or poly(butylene adipateâ€ <i>co</i> â€ŧerephthalate). Polymer Engineering and Science, 2011, 51, 1023-1032.	3.1	54
63	Water-assisted compounding of cellulose nanocrystals into polyamide 6 for use as a nucleating agent for microcellular foaming. Polymer, 2016, 84, 158-166.	3.8	53
64	Fabrication of porous synthetic polymer scaffolds for tissue engineering. Journal of Cellular Plastics, 2015, 51, 165-196.	2.4	52
65	Short cellulose nanofibrils as reinforcement in polyvinyl alcohol fiber. Cellulose, 2014, 21, 4287-4298.	4.9	51
66	The effect of nanoclay on the crystallization behavior, microcellular structure, and mechanical properties of thermoplastic polyurethane nanocomposite foams. Polymer Engineering and Science, 2016, 56, 319-327.	3.1	51
67	Fabrication of fibrous silica sponges by self-assembly electrospinning and their application in tissue engineering for three-dimensional tissue regeneration. Chemical Engineering Journal, 2018, 331, 652-662.	12.7	49
68	Fabrication of polylactic acid/polyethylene glycol ( <scp>PLA</scp> / <scp>PEG</scp> ) porous scaffold by supercritical <scp>CO</scp> <sub>2</sub> foaming and particle leaching. Polymer Engineering and Science, 2015, 55, 1339-1348.	3.1	48
69	Approaches to Fabricating Multiple-Layered Vascular Scaffolds Using Hybrid Electrospinning and Thermally Induced Phase Separation Methods. Industrial & Engineering Chemistry Research, 2016, 55, 882-892.	3.7	48
70	Microcellular and Solid Polylactide–Flax Fiber Composites. Composite Interfaces, 2009, 16, 869-890.	2.3	47
71	Development of biomimetic thermoplastic polyurethane/fibroin smallâ€diameter vascular grafts via a novel electrospinning approach. Journal of Biomedical Materials Research - Part A, 2018, 106, 985-996.	4.0	47
72	Polycaprolactone Nanofibers Containing Vascular Endothelial Growth Factor-Encapsulated Gelatin Particles Enhance Mesenchymal Stem Cell Differentiation and Angiogenesis of Endothelial Cells. Biomacromolecules, 2018, 19, 3747-3753.	5.4	47

#	Article	IF	CITATIONS
73	Fabrication of Porous Poly(ε-caprolactone) Scaffolds Containing Chitosan Nanofibers by Combining Extrusion Foaming, Leaching, and Freeze-Drying Methods. Industrial & Engineering Chemistry Research, 2014, 53, 17909-17918.	3.7	46
74	Instantaneous self-assembly of three-dimensional silica fibers in electrospinning: Insights into fiber deposition behavior. Materials Letters, 2017, 204, 45-48.	2.6	46
75	A review of thermoplastic polymer foams for functional applications. Journal of Materials Science, 2021, 56, 11579-11604.	3.7	46
76	Preparation of thermoplastic polyurethane/graphene oxide composite scaffolds by thermally induced phase separation. Polymer Composites, 2014, 35, 1408-1417.	4.6	45
77	Electrospinning Homogeneous Nanofibrous Poly(propylene carbonate)/Gelatin Composite Scaffolds for Tissue Engineering. Industrial & Engineering Chemistry Research, 2014, 53, 9391-9400.	3.7	45
78	Mechanical properties, crystallization characteristics, and foaming behavior of polytetrafluoroethylene-reinforced poly(lactic acid) composites. Polymer Engineering and Science, 2017, 57, 570-580.	3.1	44
79	Sub-critical gas-assisted processing using CO 2 foaming to enhance the exfoliation of graphene in polypropyleneÂ+ graphene nanocomposites. Polymer, 2017, 117, 132-139.	3.8	43
80	Controlling Superwettability by Microstructure and Surface Energy Manipulation on Three-Dimensional Substrates for Versatile Gravity-Driven Oil/Water Separation. ACS Applied Materials & Interfaces, 2017, 9, 37529-37535.	8.0	43
81	Programmed Release of Multimodal, Cross-Linked Vascular Endothelial Growth Factor and Heparin Layers on Electrospun Polycaprolactone Vascular Grafts. ACS Applied Materials & Interfaces, 2019, 11, 32533-32542.	8.0	43
82	Fabrication of thermoplastic polyurethane tissue engineering scaffold by combining microcellular injection molding and particle leaching. Journal of Materials Research, 2014, 29, 911-922.	2.6	42
83	Manipulating the structure and mechanical properties of thermoplastic polyurethane/polycaprolactone hybrid small diameter vascular scaffolds fabricated via electrospinning using an assembled rotating collector. Journal of the Mechanical Behavior of Biomedical Materials, 2018, 78, 433-441.	3.1	42
84	Fabrication of polycaprolactone electrospun fibers with different hierarchical structures mimicking collagen fibrils for tissue engineering scaffolds. Applied Surface Science, 2018, 427, 311-325.	6.1	42
85	Process optimization of injection molding using an adaptive surrogate model with Gaussian process approach. Polymer Engineering and Science, 2007, 47, 684-694.	3.1	41
86	A novel thermoplastic polyurethane scaffold fabrication method based on injection foaming with water and supercritical carbon dioxide as coblowing agents. Polymer Engineering and Science, 2014, 54, 2947-2957.	3.1	41
87	Mathematical modeling and numerical simulation of cell growth in injection molding of microcellular plastics. Polymer Engineering and Science, 2004, 44, 2274-2287.	3.1	40
88	Characterization and properties of electrospun thermoplastic polyurethane blend fibers: Effect of solution rheological properties on fiber formation. Journal of Materials Research, 2013, 28, 2339-2350.	2.6	40
89	Fabrication and characterization of injection molded poly (Îμ-caprolactone) and poly (Îμ-caprolactone)/hydroxyapatite scaffolds for tissue engineering. Materials Science and Engineering C, 2012, 32, 1674-1681.	7.3	39
90	Carbon nanotube (CNT) and nanofibrillated cellulose (NFC) reinforcement effect on thermoplastic polyurethane (TPU) scaffolds fabricated via phase separation using dimethyl sulfoxide (DMSO) as solvent. Journal of the Mechanical Behavior of Biomedical Materials, 2016, 62, 417-427.	3.1	39

#	Article	IF	CITATIONS
91	Fabrication of highly expanded thermoplastic polyurethane foams using microcellular injection molding and gas-laden pellets. Polymer Engineering and Science, 2015, 55, 2643-2652.	3.1	37
92	Investigation of Thermal and Thermomechanical Properties of Biodegradable PLA/PBSA Composites Processed via Supercritical Fluid-Assisted Foam Injection Molding. Polymers, 2017, 9, 22.	4.5	37
93	Intelligent Injection Molding on Sensing, Optimization, and Control. Advances in Polymer Technology, 2020, 2020, 1-22.	1.7	36
94	Crystallization measurements via ultrasonic velocity: Study of poly(lactic acid) parts. Journal of Polymer Science, Part B: Polymer Physics, 2015, 53, 700-708.	2.1	35
95	Enhancing Nanofiller Dispersion Through Prefoaming and Its Effect on the Microstructure of Microcellular Injection Molded Polylactic Acid/Clay Nanocomposites. Industrial & Engineering Chemistry Research, 2015, 54, 7122-7130.	3.7	34
96	Fabrication of triple-layered vascular scaffolds by combining electrospinning, braiding, and thermally induced phase separation. Materials Letters, 2015, 161, 305-308.	2.6	34
97	Wavy small-diameter vascular graft made of eggshell membrane and thermoplastic polyurethane. Materials Science and Engineering C, 2020, 107, 110311.	7.3	34
98	Long-term nitric oxide release for rapid endothelialization in expanded polytetrafluoroethylene small-diameter artificial blood vessel grafts. Applied Surface Science, 2020, 507, 145028.	6.1	34
99	Adaptive online quality control for injection-molding by monitoring and controlling mold separation. Polymer Engineering and Science, 2006, 46, 569-580.	3.1	33
100	Injection molding quality control by integrating weight feedback into a cascade closed-loop control system. Polymer Engineering and Science, 2007, 47, 852-862.	3.1	31
101	Influence and prediction of processing parameters on the properties of microcellular injection molded thermoplastic polyurethane based on an orthogonal array test. Journal of Cellular Plastics, 2013, 49, 439-458.	2.4	31
102	Mechanical properties, fiber orientation, and length distribution of glass fiberâ€reinforced polypropylene parts: Influence of waterâ€foaming technology. Polymer Composites, 2018, 39, 4386-4399.	4.6	31
103	In-situ ultrasonic characterization of microcellular injection molding. Journal of Materials Processing Technology, 2019, 270, 254-264.	6.3	31
104	Novel injection molding foaming approaches using gasâ€laden pellets with N <sub>2</sub> , CO <sub>2</sub> , and N <sub>2</sub> + CO <sub>2</sub> as the blowing agents. Polymer Engineering and Science, 2014, 54, 899-913.	3.1	30
105	Properties and fibroblast cellular response of soft and hard thermoplastic polyurethane electrospun nanofibrous scaffolds. Journal of Biomedical Materials Research - Part B Applied Biomaterials, 2015, 103, 960-970.	3.4	30
106	Aerogel microspheres based on cellulose nanofibrils as potential cell culture scaffolds. Cellulose, 2017, 24, 2791-2799.	4.9	30
107	A Multidomain Model of Planar Electro-Active Polymer Actuators. IEEE Transactions on Industry Applications, 2005, 41, 1142-1148.	4.9	29
108	Defect diagnosis for polymeric samples via magnetic levitation. NDT and E International, 2018, 100, 175-182.	3.7	29

7

#	Article	IF	CITATIONS
109	Surface modification of polytetrafluoroethylene (PTFE) with a heparin-immobilized extracellular matrix (ECM) coating for small-diameter vascular grafts applications. Materials Science and Engineering C, 2021, 128, 112301.	7.3	29
110	Fabrication of shish–kebab structured poly(ε-caprolactone) electrospun nanofibers that mimic collagen fibrils: Effect of solvents and matrigel functionalization. Polymer, 2014, 55, 5396-5406.	3.8	28
111	Adaptive multiobjective optimization of process conditions for injection molding using a Gaussian process approach. Advances in Polymer Technology, 2007, 26, 71-85.	1.7	27
112	Study of polystyrene/titanium dioxide nanocomposites via melt compounding for optical applications. Polymer Composites, 2007, 28, 241-250.	4.6	27
113	Morphological evolution and orientation development of stretched iPP films: Influence of draw ratio. Journal of Polymer Science, Part B: Polymer Physics, 2010, 48, 1223-1234.	2.1	27
114	Effect of carbonization temperature on mechanical properties and biocompatibility of biochar/ultra-high molecular weight polyethylene composites. Composites Part B: Engineering, 2020, 196, 108120.	12.0	27
115	Adaptive geometry and process optimization for injection molding using the kriging surrogate model trained by numerical simulation. Advances in Polymer Technology, 2008, 27, 1-16.	1.7	26
116	Enhanced performance of an expanded polytetrafluoroethylene-based triboelectric nanogenerator for energy harvesting. Nano Energy, 2019, 60, 903-911.	16.0	26
117	Axial-Circular Magnetic Levitation: A Three-Dimensional Density Measurement and Manipulation Approach. Analytical Chemistry, 2020, 92, 6925-6931.	6.5	26
118	Crystallization and thermal behavior of microcellular injection-molded polyamide-6 nanocomposites. Polymer Engineering and Science, 2006, 46, 904-918.	3.1	25
119	A new microcellular injection molding process for polycarbonate using water as the physical blowing agent. Polymer Engineering and Science, 2012, 52, 1464-1473.	3.1	25
120	Comparative study of chemical and physical foaming methods for injection-molded thermoplastic polyurethane. Journal of Cellular Plastics, 2017, 53, 373-388.	2.4	25
121	Three-dimensional numerical simulation of injection mold filling with a finite-volume method and parallel computing. Advances in Polymer Technology, 2006, 25, 247-258.	1.7	24
122	Novel foam injection molding technology using carbon dioxideâ€laden pellets. Polymer Engineering and Science, 2011, 51, 2295-2303.	3.1	24
123	Improved Processability and the Processing-Structure-Properties Relationship of Ultra-High Molecular Weight Polyethylene via Supercritical Nitrogen and Carbon Dioxide in Injection Molding. Polymers, 2018, 10, 36.	4.5	24
124	Biologically Functionalized Expanded Polytetrafluoroethylene Blood Vessel Grafts. Biomacromolecules, 2020, 21, 3807-3816.	5.4	24
125	In vitro evaluations of electrospun nanofiber scaffolds composed of poly(É›-caprolactone) and polyethylenimine. Journal of Materials Research, 2015, 30, 1808-1819.	2.6	23
126	Post-crosslinkable biodegradable thermoplastic polyurethanes: Synthesis, and thermal, mechanical, and degradation properties. Materials and Design, 2017, 127, 106-114.	7.0	23

#	Article	IF	CITATIONS
127	Polylactide/thermoplastic polyurethane/polytetrafluoroethylene nanocomposites with in situ fibrillated polytetrafluoroethylene and nanomechanical properties at the interface using atomic force microscopy. Polymer Testing, 2018, 67, 22-30.	4.8	23
128	Effects of nanoclays on the thermal stability and flame retardancy of microcellular thermoplastic polyurethane nanocomposites. Polymer Composites, 2018, 39, E1429.	4.6	23
129	Modification of 3-D Porous Hydroxyapatite/Thermoplastic Polyurethane Composite Scaffolds for Reinforcing Interfacial Adhesion by Polydopamine Surface Coating. ACS Omega, 2019, 4, 6382-6391.	3.5	23
130	Eggshell membrane and expanded polytetrafluoroethylene piezoelectricâ€enhanced triboelectric bioâ€nanogenerators for energy harvesting. International Journal of Energy Research, 2021, 45, 11053-11064.	4.5	23
131	Comprehensive study on cellular morphologies, proliferation, motility, and epithelial–mesenchymal transition of breast cancer cells incubated on electrospun polymeric fiber substrates. Journal of Materials Chemistry B, 2017, 5, 2588-2600.	5.8	22
132	Interconnected porous poly(É›-caprolactone) tissue engineering scaffolds fabricated by microcellular injection molding. Journal of Cellular Plastics, 2018, 54, 379-397.	2.4	22
133	Micro-injection molded, poly(vinyl alcohol)-calcium salt templates for precise customization of 3D hydrogel internal architecture. Acta Biomaterialia, 2019, 95, 258-268.	8.3	22
134	Dual-scale modeling and simulation of film casting of isotactic polypropylene. Journal of Plastic Film and Sheeting, 2016, 32, 239-271.	2.2	21
135	Current state of magnetic levitation and its applications in polymers: A review. Sensors and Actuators B: Chemical, 2021, 333, 129533.	7.8	21
136	Spatial orientation of nanoclay and crystallite in microcellular injection molded polyamide-6 nanocomposites. Polymer Engineering and Science, 2007, 47, 765-779.	3.1	20
137	Influence of Processing Conditions on the Morphological Structure and Ductility of Water-Foamed Injection Molded PP/LDPE Blended Parts. Frontiers in Forests and Global Change, 2017, 36, 51-74.	1.1	20
138	The effects of nanoclay and deformation conditions on the inelastic behavior of thermoplastic polyurethane foams. Polymer Testing, 2019, 79, 106043.	4.8	20
139	An improved technique for dispersion of natural graphite particles in thermoplastic polyurethane by sub-critical gas-assisted processing. Composites Science and Technology, 2019, 182, 107783.	7.8	20
140	Nanofibrous Electrospun Polymers for Reprogramming Human Cells. Cellular and Molecular Bioengineering, 2014, 7, 379-393.	2.1	18
141	Fabrication of superâ€ductile PP/LDPE blended parts with a chemical blowing agent. Journal of Applied Polymer Science, 2016, 133, .	2.6	18
142	Novel polydimethylsiloxane (PDMS) composites reinforced with three-dimensional continuous silica fibers. Materials Letters, 2018, 210, 173-176.	2.6	18
143	Expanded Polytetrafluoroethylene/Graphite Composites for Easy Water/Oil Separation. ACS Applied Materials & Interfaces, 2020, 12, 38241-38248.	8.0	18
144	Electrospun bead-in-string fibrous membrane prepared from polysilsesquioxane-immobilising poly(lactic acid) with low filtration resistance for air filtration. Journal of Polymer Research, 2020, 27, 1.	2.4	18

#	Article	IF	CITATIONS
145	Microcellular injection molding of polymers: a review of process know-how, emerging technologies, and future directions. Current Opinion in Chemical Engineering, 2021, 33, 100694.	7.8	18
146	Microcellular injection molding of recycled poly(ethylene terephthalate) blends with chain extenders and nanoclay. Journal of Polymer Engineering, 2014, 34, 5-13.	1.4	17
147	Hierarchically decorated electrospun poly( \$\$ varepsilon \$\$ ε -caprolactone)/nanohydroxyapatite composite nanofibers for bone tissue engineering. Journal of Materials Science, 2015, 50, 4174-4186.	3.7	17
148	Biocompatible graphene nanosheets grafted with poly(2-hydroxyethyl methacrylate) brushes via surface-initiated ARGET ATRP. RSC Advances, 2016, 6, 35641-35647.	3.6	17
149	Microcellular poly(hydroxybutyrateâ€ <i>co</i> â€hydroxyvalerate)â€hyperbranched polymer–nanoclay nanocomposites. Polymer Engineering and Science, 2011, 51, 1815-1826.	3.1	16
150	Effect of a cross-linking agent on the foamability of microcellular injection molded thermoplastic polyurethane. Journal of Cellular Plastics, 2017, 53, 407-423.	2.4	16
151	Modeling and characterization of crystallization during rapid heat cycle molding. Polymer Testing, 2018, 71, 182-191.	4.8	16
152	Ethanol-lubricated expanded-polytetrafluoroethylene vascular grafts loaded with eggshell membrane extract and heparin for rapid endothelialization and anticoagulation. Applied Surface Science, 2020, 511, 145565.	6.1	16
153	A biomimetic basement membrane consisted of hybrid aligned nanofibers and microfibers with immobilized collagen IV and laminin for rapid endothelialization. Bio-Design and Manufacturing, 2021, 4, 171-189.	7.7	16
154	Fabrication and modification of wavy multicomponent vascular grafts with biomimetic mechanical properties, antithrombogenicity, and enhanced endothelial cell affinity. Journal of Biomedical Materials Research - Part B Applied Biomaterials, 2019, 107, 2397-2408.	3.4	15
155	Poly[(Butyl acrylate)- <i>co</i> -(butyl methacrylate)] as Transparent Tribopositive Material for High-Performance Hydrogel-Based Triboelectric Nanogenerators. ACS Applied Polymer Materials, 2020, 2, 5219-5227.	4.4	15
156	Investigation of crystallization behavior of solid and microcellular injection molded polypropylene/nano-calcium carbonate composites using carbon dioxide as a blowing agent. Journal of Cellular Plastics, 2013, 49, 459-475.	2.4	14
157	Fabrication of biocompatible nanohybrid shish-kebab-structured carbon nanotubes with a mussel-inspired layer. RSC Advances, 2016, 6, 101660-101670.	3.6	14
158	Injection and injection compression molding of ultraâ€highâ€molecular weight polyethylene powder. Polymer Engineering and Science, 2019, 59, E170.	3.1	14
159	Microcellular injection molding process for producing lightweight thermoplastic polyurethane with customizable properties. Frontiers of Mechanical Engineering, 2018, 13, 96-106.	4.3	13
160	Preparation of fastâ€degrading poly(lactic acid)/soy protein concentrate biocomposite foams via supercritical CO <sub>2</sub> foaming. Polymer Engineering and Science, 2019, 59, 1753-1762.	3.1	13
161	Development of a rheoâ€dielectric sensor for online shear stress measurement during the injection molding process. Polymer Engineering and Science, 2010, 50, 61-68.	3.1	12
162	Fabrication of super ductile polymeric blends using microcellular injection molding. Manufacturing Letters, 2014, 2, 64-68.	2.2	12

#	Article	IF	CITATIONS
163	Novel foaming method to fabricate microcellular injection molded polycarbonate parts using sodium chloride and active carbon as nucleating agents. Polymer Engineering and Science, 2015, 55, 1634-1642.	3.1	12
164	Ultrasonicationâ€Induced Modification of Hydroxyapatite Nanoparticles onto a 3D Porous Poly(lactic) Tj ETQq0 and Engineering, 2019, 304, 1900081.	0 0 rgBT / 3.6	Overlock 10 T 12
165	The Microcellular Injection Molding of Low-Density Polyethylene (LDPE) Composites. Polymer-Plastics Technology and Engineering, 2010, 49, 1339-1346.	1.9	11
166	Comparisons of microcellular polylactic acid parts injection molded with supercritical nitrogen and expandable thermoplastic microspheres: Surface roughness, tensile properties, and morphology. Journal of Cellular Plastics, 2013, 49, 33-45.	2.4	11
167	Microcellular injection molding of <i>in situ</i> modified poly(ethylene terephthalate) with supercritical nitrogen. Polymer Engineering and Science, 2014, 54, 2739-2745.	3.1	11
168	Endogenous biological factors modulated by substrate stiffness regulate endothelial differentiation of mesenchymal stem cells. Journal of Biomedical Materials Research - Part A, 2018, 106, 1595-1603.	4.0	11
169	Effect of centerline distance on mixing of a Non-Newtonian fluid in a cavity with asymmetric rotors. Physics of Fluids, 2019, 31, 021205.	4.0	11
170	Oriented polyvinyl alcohol films using short cellulose nanofibrils as a reinforcement. Journal of Applied Polymer Science, 2015, 132, .	2.6	10
171	Injection molding of delaminationâ€free ultraâ€highâ€molecularâ€weight polyethylene. Polymer Engineering and Science, 2019, 59, 2313-2322.	3.1	10
172	Semitransparent poly(styrene-r-maleic anhydride)/alumina nanocomposites for optical applications. Journal of Applied Polymer Science, 2007, 105, 2728-2736.	2.6	9
173	Chaotic mixing in a single-screw extruder with a moving internal baffle. Polymer Engineering and Science, 2014, 54, 198-207.	3.1	9
174	Numerical simulation on residual thickness of pipes with curved sections in waterâ€assisted coâ€injection molding. Journal of Applied Polymer Science, 2015, 132, .	2.6	9
175	Experimental study of penetration interfaces in the overflow fluid-assisted co-injection molding process. Journal of Polymer Engineering, 2016, 36, 139-148.	1.4	9
176	Effects of nucleation and stereocomplex formation of poly(lactic acid). Journal of Polymer Engineering, 2016, 36, 673-679.	1.4	9
177	Mechanical properties and thermal characteristics of poly(lactic acid) and paraffin wax blends prepared by conventional melt compounding and sub-critical gas-assisted processing (SGAP). European Polymer Journal, 2018, 98, 262-272.	5.4	9
178	Residual wall thickness of waterâ€powered projectileâ€assisted injection molding pipes. Polymer Engineering and Science, 2019, 59, 295-303.	3.1	9
179	Expanded Poly(tetrafluoroethylene) Blood Vessel Grafts with Embedded Reactive Oxygen Species (ROS)-Responsive Antithrombogenic Drug for Elimination of Thrombosis. ACS Applied Materials & Interfaces, 2020, 12, 29844-29853.	8.0	9
180	Modeling and prediction of morphology and crystallinity for cylindricalâ€shaped crystals during polymer processing. Polymer Engineering and Science, 2010, 50, 1226-1235.	3.1	8

#	Article	IF	CITATIONS
181	The degradation rate of polyanhydride (poly(sebacic acid), diacetoxy terminated, PSADT). Journal Wuhan University of Technology, Materials Science Edition, 2013, 28, 793-797.	1.0	8
182	Numerical study of mixing dynamics inside the novel elements of a corotating nontwin screw extruder. Advances in Polymer Technology, 2018, 37, 2478-2496.	1.7	8
183	Nonâ€linear rheological response as a tool for assessing dispersion in polypropylene/polycaprolactone/clay nanocomposites and blends made with subâ€critical gasâ€assisted processing. Polymer Engineering and Science, 2020, 60, 55-60.	3.1	8
184	Core-Shell Rubber Modified Microcellular Polyamide-6 Composite. Journal of Cellular Plastics, 2004, 40, 383-395.	2.4	7
185	Flash. Polymer Engineering and Science, 2006, 46, 241-247.	3.1	7
186	Process optimization and effects of material properties on numerical prediction of warpage for injection molding. Advances in Polymer Technology, 2008, 27, 199-216.	1.7	7
187	Comparisons of microcellular polylactic acid parts injection molded with supercritical nitrogen and expandable thermoplastic microspheres: Surface roughness, tensile properties, and morphology. Journal of Cellular Plastics, 2012, 48, 433-444.	2.4	7
188	Expanded polytetrafluoroethylene/silk fibroin/salicin vascular graft fabrication for improved endothelialization and anticoagulation. Applied Surface Science, 2021, 542, 148610.	6.1	7
189	Fabrication of Poly(lactic acid)/Silkworm Excrement Composite with Enhanced Crystallization, Toughness and Biodegradation Properties. Journal of Polymers and the Environment, 2020, 28, 295-303.	5.0	6
190	Characterization of polymer materials using magnetic levitation. Journal of Materials Research, 2020, 35, 1182-1189.	2.6	6
191	Evaluating the gas-laden ability of polymer melt under atmospheric conditions using a modified torque rheometer. Journal of Cellular Plastics, 0, , 0021955X2199735.	2.4	6
192	Effects of expandable graphite on the flame-retardant and mechanical performances of rigid polyurethane foams. Journal of Physics Condensed Matter, 2022, 34, 084002.	1.8	6
193	Enhancement of mixing by different baffle arrays in cavity flows. Chemical Engineering Science, 2015, 137, 837-851.	3.8	5
194	Fracture toughness assessment of polypropylene random copolymer with multiple stress modes using the essential work of fracture theory. Polymer Testing, 2015, 41, 73-81.	4.8	5
195	Experimental study on the penetration interfaces of pipes with different cross-sections in overflow water-assisted coinjection molding. Journal of Applied Polymer Science, 2016, 133, n/a-n/a.	2.6	5
196	Improving the processibility and mechanical properties of poly(lactic acid)/linear lowâ€density polyethylene/paraffin wax blends by subcritical gasâ€assisted processing. Polymer Engineering and Science, 2018, 58, 2320-2331.	3.1	5
197	Core/shell structure of electrospun polycarbonate nanofibers. Polymer Testing, 2018, 70, 498-502.	4.8	5
198	Breakup of a Viscoelastic Droplet in Co-Rotating Non-Twin Screw Channels. Industrial & Engineering Chemistry Research, 2020, 59, 15075-15086.	3.7	5

#	Article	IF	CITATIONS
199	Viscosity characterization and flow simulation and visualization of polytetrafluoroethylene paste extrusion using a green and biofriendly lubricant. Polymer Engineering and Science, 2021, 61, 1050-1065.	3.1	5
200	Cell morphologies, mechanical properties, and fiber orientation of glass fiber-reinforced polyamide composites: Influence of subcritical gas-laden pellet injection molding foaming technology. Physics of Fluids, 2022, 34, .	4.0	5
201	Physical shish-kebab modification vs. chemical surface coating on expanded polytetrafluoroethylene vascular grafts for enhanced endothelial cell adhesion. Materials and Design, 2022, 220, 110889.	7.0	5
202	Structural evolution of uniaxial tensile-deformed injection molded poly(É›-caprolactone)/hydroxyapatite composites. Polymer Composites, 2017, 38, 1771-1782.	4.6	4
203	Comparative study of crystallization and lamellae orientation of isotactic polypropylene by rapid heat cycle molding and conventional injection molding. E-Polymers, 2017, 17, 71-81.	3.0	4
204	Stereocomplex formation in injection-molded poly(L-lactic acid)/poly(D-lactic acid) blends. Journal of Polymer Engineering, 2019, 39, 279-286.	1.4	4
205	A Visualization of Flow Patterns of Viscoelastic Fluid Partially Filled in a Coâ€Rotating Nontwin Screw Extruder. Polymer Engineering and Science, 2019, 59, E24.	3.1	4
206	A multi-scale numerical simulation of the crystallisation and temperature field of glass. Molecular Physics, 2017, 115, 3024-3032.	1.7	3
207	Subcritical gasâ€assisted processing of ethylene vinyl alcohol + nanoclay composites. Polymer Composites, 2020, 41, 1584-1594.	4.6	3
208	Topological Chaos by Pseudo-Anosov Map in Cavity Laminar Mixing. Journal of Computational and Nonlinear Dynamics, 2015, 10, .	1.2	2
209	A Numerical Simulation of Enhanced Mixing of a Nonâ€Newtonian Fluid in a Cavity with Asymmetric Nonâ€īwin Rotors. Macromolecular Theory and Simulations, 2018, 27, 1800021.	1.4	2
210	Applications of Core Retraction in Manufacturing Low-Density Polypropylene Foams with Microcellular Injection Molding. Frontiers in Forests and Global Change, 2018, 37, 1-20.	1.1	2
211	Evaluation of Mixing Performance in Baffled Screw Channel Using Lagrangian Particle Calculations. Advances in Polymer Technology, 2017, 36, 86-97.	1.7	1
212	Effect of longitudinal periodic length on chaotic mixing in a lid-driven cavity flow system. Journal of Non-Newtonian Fluid Mechanics, 2018, 261, 81-98.	2.4	1
213	Sub-critical gas-assisted processing of ethylene vinyl alcohol + nanoclay composites. AIP Conference Proceedings, 2019, , .	0.4	1
214	Effect of alkyl group on the chain extension of phosphites in polylactide. Journal of Vinyl and Additive Technology, 2019, 25, 144-148.	3.4	1
215	Dual-Scale Modeling and Simulation of Skin Layer Thickness in Injection Molding with Variable Mold Temperatures. Journal of Computational and Theoretical Nanoscience, 2016, 13, 7125-7136.	0.4	0